UNDERWATER IMAGE DESCATTERING AND QUALITY ASSESSMENT

Huimin Lu[1,], Yujie Li[2], Xing Xu[3], Li He[4], Yun Li[2], Donald G. Dansereau[5], Seiichi Serikawa[1]*

[1]Kyushu Institute of Technology, Japan
[2]Yangzhou University, China
[3]University of Electrical Science and Technology of China, China
[4]Qualcomm R&D Center, USA
[5]Queensland University of Technology, Australia
[*]luhuimin@ieee.org

ABSTRACT

Vision-based underwater navigation and object detection requires robust computer vision algorithms to operate in turbid water. Many conventional methods aimed at improving visibility in low turbid water. In this paper, we propose a novel contrast enhancement to enhance high turbid underwater images using descattering and color correction. The proposed enhancement method removes the scatter and preserves colors. In addition, as a rule to compare the performance of different image enhancement algorithms, a more comprehensive image quality assessment index Q_u is proposed. The index combines the benefits of SSIM index and color distance index. Experimental results show that the proposed approach statistically outperforms state-of-the-art general purpose underwater image contrast enhancement algorithms. The experiment also demonstrated that the proposed method performs well for image classification.

Index Terms— Contrast enhancement, image quality assessment, underwater imaging, ocean optics

1. INTRODUCTION

Underwater robots have been limited by the need to recognize underwater minerals, fishes, etc. In the last two decades, sonar has been widely used to detect and recognize objects in oceans. However, for short-range identification, sonar yields low-resolution images due to the limitation of the low quality acoustic aperture. Consequently, vision sensors are typically used for detection and classification [1].

Different from natural images, underwater optical images suffer from poor visibility due to the medium, which causes scattering and absorption. Especially in shallow water, large suspended particles cause scatter in the light-path. Color distortion occurs because different wavelengths are attenuated to different degrees in water. This random attenuation of light causes haziness because the light backscattered by water along the line of sight degrades image contrast considerably [2].

In recent years, researchers have developed several methods to enhance underwater images. Schechner et al. exploited a polarization filter to compensate for visibility degradation [3], while Bazeille et al. proposed an image pre-processing framework for enhancing images in turbid water [4]. Fattal designed a color lines method to estimate the turbidity of haze, and then used a Markov Random Fields model to recover clean images [5]. He et al. proposed the dark channel prior to estimating the depth map [6]. Nicholas et al. used the dark channel prior and a graph-cut method rather than soft matting to refine the depth map [7]. Martin et al. combined a stereo matching and light attenuation model to recover visibility under water [8]. Lee et al. proposed a stereo image defogging method by using an estimation of scattering parameters through a stereo image pair [9]. Tarel et al. used a median dark channel prior method in a turbid medium to recover a clear image [10]. Chiang et al. investigated the effect of variations in wavelength on underwater imaging using the dark channel prior model [11]. However, the aforementioned approaches cannot perform well for high-turbidity underwater images. In high-turbidity water, it is difficult to obtain the ambient light and fine depth map using the conventional methods.

In this paper, we propose a contrast enhancement based on a joint normalized image and color correction. Furthermore, we explore a new index to measure the enhanced images. The organization of the remainder of this paper is as follows. In Section 2, we present the contrast enhancement method. In Section 3, we propose Q_u for indexing. Experimental results are given in Section 4. Finally, we conclude the paper in Section 5.

2. CONTRAST ENHANCEMENT

Underwater dark channel prior-based image enhancement methods use a depth map to remove scatter. However, if the input images are highly distorted, the real depth maps are

with obviously blurring. To this end, we propose a guidance image filtering method to refine the depth map.

2.1. Underwater Imaging Model

Underwater imaging models generally follow a standard attenuation model to accommodate wavelength attenuation coefficients. For underwater imaging, the observed irradiance is a linear combination attenuated in the route of sight and the scattered ambient light. Therefore, a modified Koschmieder model [12] is employed for underwater lighting conditions.

The modified Koschmieder model can be expressed as follows:

$$I^c(x) = J^c(x)e^{-\eta d(x)} + \rho(x)\cdot J^c(x)(1-e^{-\eta d(x)}), c \in \{r,g,b\} \quad (1)$$

where $J^c(x)$ is the real scene at water depth $D(x)$, $\rho(x)$ is the normalized radiance of a scene point, $d(x)$ is the distance from the scene point to the camera, and η is the total beam attenuation coefficient which is nonlinear and dependent on the wavelength.

The proposed method is based on [13]. We found that turbid underwater images mostly exhibit dark qualities. The minimum operation is suitable for reducing the halo effect when estimating the rough transmission. Thus, the underwater dark channel priors (UDCP) can be defined as:

$$\tilde{d}(x) = \min_{\Re(m,n)}\left(\min_{c\in\{r,b\}} \frac{I^c(x)}{\rho(x)J^c(x)}\right), c \in \{r,b\} \quad (2)$$

where $\Re$ is a square window of size 5 × 5. For each pixel located at position (m, n) in the square patch $\Re$, the values from the red and blue channels are compared, and the lower value is selected. The proposed method can prevent the halo effect around occlusion boundaries. Accordingly, the coarse estimate of transmission is obtained as follows:

$$d(x) = 1 - \omega\tilde{d}(x), \quad (3)$$

where $\omega = 0.8$ for most scenes.

2.2. Depth Map Refinement by Guidance Image

In Section 2.1, we discussed the rough estimation of the coarse depth map. However, its depth map contains mosaic effects and blurring, which yields less accurate results. Therefore, we have developed a joint filter to reduce such mosaic effects. The normalized image is obtained as follows:

$$I_f^c(x) = \begin{cases} \dfrac{I^c(x) - I^c_{\min}(x)}{I^c_{\max}(x) - I^c_{\min}(x)}, & if\ 0 < I^c(x) < 1 \\ 0, & if\ 0 > I^c(x) \\ 1, & if\ 1 < I^c(x) \end{cases}, c \in \{r,g,b\} \quad (4)$$

The refinement of the joint filtered is first performed under the guidance image $I_f^c(x)$. Here, let $d_p(x)$, $d_q(x)$, $I^c_{f,p}(x)$ and $I^c_{f,q}(x)$ be the intensity value at the pixel p, q of the depth map and the guidance image, respectively, while w_k is the kernel window centered at pixel k. The refined depth map is then formulated as:

$$R(x) = \frac{1}{\sum_{q\in w_k} W_{pq}(I_f^c(x))} \sum_{q\in w_k} W_{pq}(I_f^c(x)) d_q(x) \quad (5)$$

where the kernel weight function $W_{G_{pq}}(I_f^c(x))$ is expressed as:

$$W_{pq}(I_f^c(x)) = \frac{1}{|w|^2} \sum_{k:(p,q)\in w_k} \left(1 + \frac{(I^c_{f,p}(x) - \mu_k)(I^c_{f,q}(x) - \mu_k)}{\sigma_k^2 + \varepsilon}\right) \quad (6)$$

where μ_k and σ_k^2 are the mean and variance of the guidance image in the local window w_k, and $|w|$ is the number of pixels in this window. After the refined depth map is obtained, we can recover the real scene using the underwater dark channel prior descattering model. Fig.1 shows the result of refined depth map.

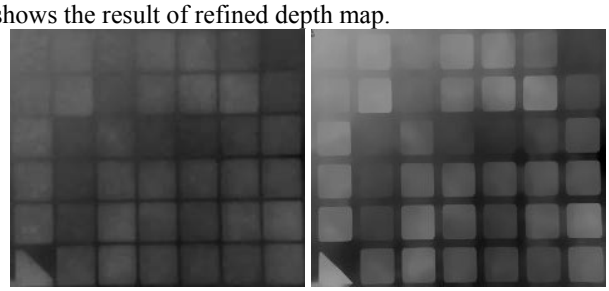

(a) (b)

Fig.1. Depth map refinement. (a) Rough depth map by UDCP [13]. (b) Refined depth map by our method.

2.3. Color Correction

After descattering, the colors are seriously distorted. We use the physical spectral characteristics based color correction method to address this distortion. We take the chromatic transfer function τ to weight the light from the surface to a given depth of objects as follows:

$$\tau_\lambda = \frac{E_\lambda^{surface}}{E_\lambda^{object}} \quad (7)$$

where the transfer function τ at wavelength λ is derived from the irradiance of the surface $E_\lambda^{surface}$ by the irradiance of the object E_λ^{object}. According to the spectral response of the RGB camera, we convert the transfer function to the RGB domain as follows:

$$\tau_{RGB} = \int_{400nm}^{725nm} \tau_\lambda \cdot C_c(\lambda) d\lambda, c \in \{r,g,b\} \quad (8)$$

where the weighted RGB transfer function is τ_{RGB}, and $C_c(\lambda)$ is the underwater spectral characteristic function of the color band c, $c \in \{r,g,b\}$. Finally, the corrected image is gathered from the weighted RGB transfer function as follows:

$$J_\lambda^c(x) = \nu_{RGB} \cdot \hat{J}_\lambda^c(x) \cdot \tau_{RGB} \quad (9)$$

where $J_\lambda^c(x)$ and $\hat{J}_\lambda^c(x)$ are the color corrected and uncorrected images respectively. ν_{RGB} is the spectral power distribution transfer function. It can be measured by spectrometer [18].

3. QUALITY ASSESSMENT RULE

There are many methods for underwater image enhancement; however, there are few image quality assessment rules for underwater images [21]. We typically conducted quantitative analysis, primarily from the perspective of mathematical statistics and the statistical parameters for underwater image quality assessment. This analysis includes contrast to noise ratio (CNR) [14], structural similarity (SSIM) [15], and color distance [16]. Here, we introduce a new quality assessment rule for underwater images. First, we recall some conventional image quality indexes. The CNR is similar to the signal-to-noise ratio (SNR) and robust in measuring hazy images. The value of the CNR [14] is between 0 (worst) and 100 (best).

Let μ_A, σ_A, and σ_{AB} respectively as the mean of image A, the variance of image A, the covariance of images A and B, respectively. The SSIM [15] is given as follows:

$$SSIM(A,B) = \frac{(2\mu_A\mu_B + C_1)(2\sigma_{AB} + C_2)}{(\mu_A^2 + \mu_B^2 + C_1)(\mu_A^2 + \mu_B^2 + C_2)} \tag{10}$$

where C_1, and C_2 are the small constants. SSIM is the structural similarity (values are between 0 (worst) and 1 (best)).

The metric ΔE represents the Euclidean distance between two colors in the *Lab* color space. It is calculated from their L, a, and b values as follows:

$$\Delta E(A,B) = \sqrt{(L_A - L_B)^2 + (a_A - a_B)^2 + (b_A - b_B)^2} \tag{11}$$

where smaller of ΔE values indicate greater similarity between images A and B. The inverse normalized color distance is defined as:

$$\overline{\Delta E(A,B)} = 1 - \frac{\Delta E(A,B)}{E_{\max}} \tag{12}$$

where $E_{\max}$ is the maximum color distance value. The values of $\overline{\Delta E}$ are between 0 (worst) to 1 (best).

Although SSIM performs well for measuring the structural similarity of images, there is no color information for comparison. Thus, we propose a comprehensive image quality index Q, which is defined as follows:

$$Q_u = \alpha SSIM(A,B) + \beta \overline{\Delta E(A,B)} \tag{13}$$

where α, β are the parameters. Here, we set $\alpha = \beta = 0.5$. The proposed Q_u can evaluate the similarity of both the structures and colors of images.

4. EXPERIMENTS AND DISCUSSIONS

The performance of the proposed algorithm was evaluated objectively and subjectively by utilizing ground-truth color patches. Both results demonstrate the superior scatter removal and color balancing capabilities of the proposed method over other methods. In our experiment, we compared the proposed method to recent state-of-the-art methods. Here, we selected the best parameters for each method. The computer used was equipped with Windows 8.1 and four Intel Core i7 (2.0 GHz) CPUs with 8 GB RAM.

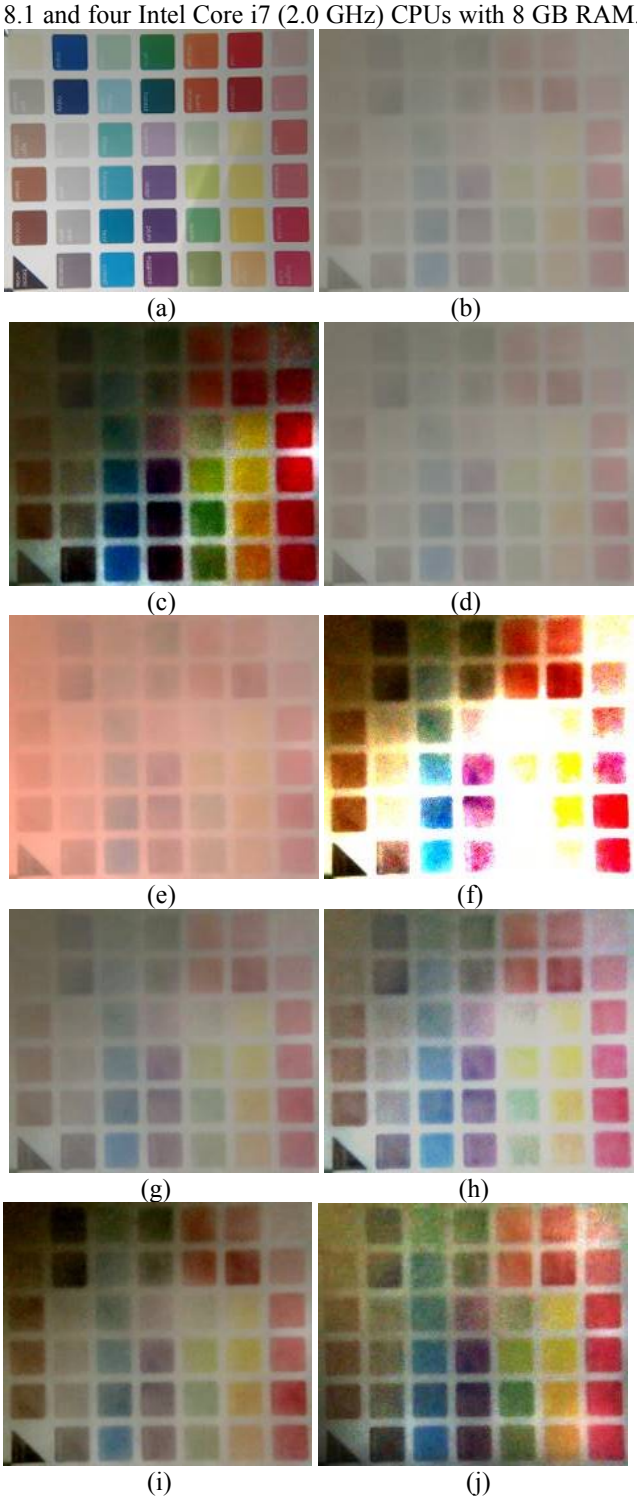

Fig.2. Simulation results of different methods in a water tank. (a) clean water image; (b) 200 mg/L turbidity water image; (c) He's method; (d) Nicholas's method; (e) Chiang's method; (f) Fattal's method; (g) Tarel's method; (h) Gibson's method; (i) Lee's method; (j) Proposed method.

In the experiment, we first captured the image of a color chart in clean water. We then added deep-sea soil to the water (from 100mg/L to 500mg/L). Fig. 2 shows the simulation results obtained using the different methods in the water tank with a turbidity of 200 mg/L.

As seen in Fig.2, Chiang's [11], and Fattal's [5] methods cause color distortion. Some scatter remained in the resulting images of Nicholas's [7] and Tarel's [10] methods. He's [6], and Lee's [9] methods cause inhomogeneous scatter (right-upper corner of the resulting images are too dark). While the result of Gibson's [17] method yields additional noise. As shown in Fig. 2(j), the proposed method removes scatter and recovers colors effectively.

In addition to the visual analysis mentioned above, we conducted quantitative analysis, primarily from the perspective of mathematical statistics and the statistical parameters of the images (Table 1). This analysis includes CNR, SSIM, inverse color distance $\overline{\Delta E}$, and Q_u. Table 1 shows the numerical results of CNR, SSIM, Color Distance and Q_u on several images. The results indicate that the proposed approach works well for scatter removal.

Table 1. Comparative Analysis of Different Enhancement Methods (Figure 2).

Methods	CNR	SSIM	$\overline{\Delta E}$	Q_u
He et al [6]	75.6850	0.5121	0.8621	0.6871
Nicholas et al [7]	63.2756	0.5918	0.9571	0.7745
Chiang et al [11]	56.0769	0.6014	0.9865	0.7940
Fattal et al [5]	66.1249	0.5373	0.9727	0.7550
Trael et al [10]	85.8001	0.6488	0.9555	0.8022
Gibson et al [17]	45.8750	0.7077	0.9756	0.8417
Lee et al [9]	90.1283	0.6535	0.9810	0.8173
Proposed	**98.0757**	**0.7110**	**0.9883**	**0.8497**

We also compared the Q_u of different methods in different scattered turbidity water. As seen in Fig.3, the average value of Q_u of the proposed method improved approximately 0.01 over the value of the best of traditional methods. Note that Fattal's method cannot remove the heavy scattered image, because the ambient light cannot be calculated by color lines.

In the second experiment, in order to certify the utility of the proposed method, we compared the classification accuracy of recently most used classification methods [18, 19]. The result is shown in Fig.4. In this experiment, we used 7330 images from the database of Japan Agency for Marine-Earth Science and Technology [20]. Images are manually classified into four classes (squid, crab, shark and minerals). We chose 5330 images for training and 2000 images for classification. From Fig.4 we can find that the proposed method can improve all of the popular classification algorithms. The average accuracy rate is improved about 1.5%. We also can conclude that the proposed method can be well applied in CNN-based classification applications.

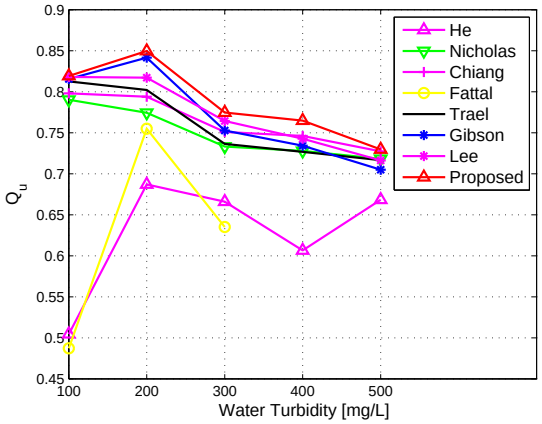

Fig.3. Comparison results of underwater enhancement methods in different water turbidity.

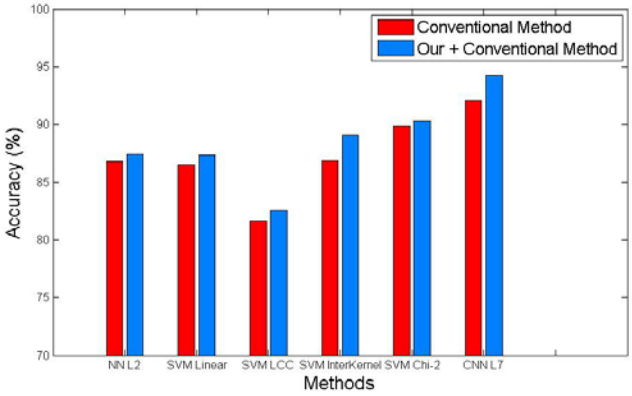

Fig.4. Comparison results of effectiveness of the proposed method in conventional classification methods

5. CONCLUSION

In this paper, we have explored and successfully implemented contrast enhancement techniques for images in high turbid water. We have proposed a joint normalized filter to refine the coarse depth map that outperforms conventional methods. Moreover, we have proposed a more comprehensive image quality assessment index that can measure the underwater image quality better than the traditional indexes. In future, we plan to design new deep learning-based algorithms for inhomogeneous scatter removal.

6. ACKNOWLEDGEMENT

This work was supported by JSPS KAKENHI (No.15F15077), Research Fund of Chinese Academy of Sciences (No.MGE2015KG02), Research Fund of State Key Laboratory of Ocean Engineering in Shanghai Jiaotong University (1315; 1510).

7. REFERENCES

[1] H. Lu, Y. Li, L. Zhang, and S. Serikawa, "Contrast enhancement for images in turbid water," *Journal of Optical Society of America A*, vol.32, no.5, pp.886-893, 2015.

[2] S. Serikawa, and H. Lu, "Underwater image dehazing using joint trilateral filter," *Computers & Electrical Engineering*, vol.40, no.1, pp.41-50, 2014.

[3] Y. Y. Schechner, and N. Karpel, "Recovery of underwater visibility and structure by polarization analysis," *IEEE Journal of Oceanic Engineering* vol.30, no.3, pp. 570–587, 2005.

[4] S. Bazeille, I. Quidu, L. Jaulin, and J. P. Malkasse, "Automatic underwater image pre-processing," in Proc. of Caracterisation Du Milieu Marin (CMM '06), pp. 1–8, 2006.

[5] R. Fattal, "Dehazing using color-lines," *ACM Transaction on Graphics*, vol.34, no.1, pp. 1–10, 2014.

[6] K. He, J. Sun, and X. Tang, "Single image haze removal using dark channel prior," *IEEE Transactions on Pattern Analysis and Machine Intelligence*, vol.33, no.12, pp. 2341–2353, 2011.

[7] C.-B Nicholas, M. Anush, and R. M. Eustice, "Initial results in underwater single image dehazing," in Proc. of IEEE OCEANS, pp. 1–8, 2010.

[8] M. Roser, M. Dunbabin, and A. Geiger, "Simultaneous underwater visibility assessment, enhancement and improved stereo," in Proc. of IEEE ICRA, pp.3840-3847, 2014.

[9] Y. Lee, K. Gibson, Z. Lee, and T. Nguyen, "Stereo image defogging," in Proc. of IEEE ICIP, pp.5427-5431, 2014.

[10] J-P. Tarel, N. Hautiere, L. Caraffa, A. Cord, H. Halmaoui, and D. Gruyer, "Vision enhancement in homogeneous and heterogeneous fog," *IEEE Intelligent Transportation Systems Magazine*, vol.4, no.2, pp.6-20, 2012.

[11] J. Y. Chiang, Y. C. Chen, "Underwater image enhancement by wavelength compensation and dehazing," *IEEE Transactions on Image Processing*, vol.21, no.4, pp. 1756–1769, 2012.

[12] H. Koschmieder, "Theorie der horizontalen sichtweite," In Beitrage zur Physik der freien Atmosphare, 1924.

[13] H. Lu, Y. Li, and S. Serikawa, "Underwater image enhancement using guided trigonometric bilateral filter and fast automatic color correction," In Proc. of ICIP, pp.3412-3416, 2013.

[14] M. Chambah, D. Semani, A. Renouf, P. Courtellemont, and A. Rizzi, "Underwater color constancy: enhancement of automatic live fish recognition," In Proc. of SPIE, vol.5293, pp.157–168, 2004.

[15] Z. Wang, A. C. Bovik, H. R. Sheikh, and E. P. Simoncelli, "Image quality assessment: From error visibility to structural similarity," *IEEE Transactions on Image Processing*, vol.13, no.4, pp. 600–612, 2004.

[16] M. Bertalmio, V. Caselles, E. Provenzi, and A. Rizzi, "Perceptual color correction through vibrational techniques," *IEEE Transactions on Image Processing*, vol.16, no.4, pp.1058–1072, 2007.

[17] K.B. Gibson, D.T. Vo, and T.Q. Nguyen, "An investigation of dehazing effects on image and video coding," *IEEE Transactions on Image Processing*, vol.21, no.2, pp. 662–673, 2012.

[18] Vision Lab Features Library, http://www.vlfeat.org/

[19] A. Krizhevsky, I. Sutskever, and G. Hinton, "ImageNet classification with deep convolutional neural networks," In Proc. of NIPS, pp.1-9, 2012.

[20] Japan Agency for Marine-Earth Science and Technology, http://www.jamstec.go.jp/

[21] K. Panetta, C. Gao, and S. Agaian, "Human visual system inspired underwater image quality measures," *IEEE Journal of Oceanic Engineering*, pp.1-11, 2015.